

# Unsteady-state heat transfer and mixing of a heat carrier in a heat exchanger with flow twisting

L. A. ASHMANTAS, B. V. DZYUBENKO, G. A. DREITSER and M. D. SEGAL

Institute of Physicotechnical Problems of Power Engineering, Lithuanian Academy of Sciences,  
233684, Kaunas, U.S.S.R.

(Received 15 November 1983)

**Abstract**—The problem of unsteady-state heat transfer is considered in a homogenized formulation with regard for the interchannel mixing in a heat exchanger with helical oval-profiled tubes. The axisymmetric temperature fields in the intertube space with increasing and decreasing rate of energy release and constant air flow rate have been studied theoretically and experimentally. The procedures of calculation and experiment are developed and dimensionless relations are suggested for the transport coefficients, required for the closure of a system of differential equations which describe the unsteady-state flow in a bundle of helical tubes. The effect of the nonsteady character of the process on the transport coefficients has been revealed.

## 1. INTRODUCTION

A HEAT exchanging apparatus with a longitudinally streamlined bundle of helical tubes [1] possesses favourable characteristics. When a heat carrier flows through the intertube space of such a heat exchanger, the helical tubes provide spiral twisting of the flow, leading to a substantial increase in the flow transport properties [2, 3] as compared with a bundle of straight tubes. For a thermohydraulic calculation of such an apparatus one needs dimensionless relations which would describe heat transfer and heat-carrier mixing both in steady- and unsteady-state conditions of the process of heating. While heat transfer and gas mixing in bundles of helical tubes under steady-state conditions have been studied to a quite satisfactory extent [1-6], the studies of unsteady-state heat transfer and mixing are virtually nonexistent. Therefore, the researchers are confronted with the task of investigating the unsteady-state heat transfer and mixing in the conditions of nonuniform heat supply along the radius of a bundle of helical tubes.

As is known, the calculation of unsteady-state heat transfer involves the solution of conjugate problems and thereby meets with insurmountable difficulties associated, first of all, with the impossibility of obtaining a closed system of equations which describes a turbulent unsteady-state flow, because of the absence of experimental data on the turbulent flow structure during the change in the wall temperature with respect to time. The authors of refs. [7, 8] have suggested the methods for the investigation of unsteady heat transfer which are based on the solution of conjugate problems with a one-dimensional description of the processes occurring in the heat carrier. They consider the heat conduction equation for the channel and one-dimensional equations of motion, energy and continuity. The system becomes closed if the

dimensionless equations are known for the quantities  $\alpha$  and  $\xi$  which are determined from the experiment. They have suggested the relations for  $\alpha$  and  $\xi$  for unsteady-state heat transfer in tubes and have shown that, with the constant flow rate of the heat carrier, a change in the wall temperature and in the heat flux with respect to time affects the heat transfer coefficient due to a change in the turbulent flow structure and to the superposition of the unsteady heat conduction on the quasi-steady convective heat transfer. Their dimensionless equations of unsteady heat transfer do not explicitly contain time in the form of the numbers  $Fo = at/d^2$  or  $Ho = ut/d$ , etc. [7], since these have been obtained under the assumption that the unsteady heat transfer differs from the quasi-steady only because of the different temperature profiles in the wall layer with thickness  $\gamma d/2$ , where  $\gamma(Pr) \ll 1$ ,  $\gamma$  is the constant of proportionality. In this case, the difference of the unsteady heat transfer coefficient from the quasi-steady one is dictated not by the laws of change of the boundary conditions in time, but only by their first derivatives ( $\partial T_w/\partial \tau$ ,  $\partial G/\partial \tau$ ) or by respective dimensionless parameters involving these derivatives.

An efficient means of the description of gas motion in a bundle with a great number of tubes has turned out to be the model of flow of a homogenized medium. It has been used with a great deal of success for the calculation of heat-carrier temperature fields in steady-state operating conditions [2, 3, 5]. When this model is applied to the unsteady heat transfer and mixing, then, along with the equations of motion, energy, continuity and state, it is necessary that the equation describing the temperature distribution in helical tubes (in the 'solid phase') be also considered. Then in the case of axisymmetric nonuniform heat release in the cross-section of a helical tube bundle, the unsteady motion of a homogenized medium will be described in a general

## NOMENCLATURE

$a$	thermal diffusivity
$c$	heat capacity
$d$	maximum dimension of the oval profile of a tube
$d_e$	equivalent diameter
$d_k$	bundle diameter
$D_t$	effective coefficient of turbulent diffusion
$F$	flow area
$Fo$	Fourier number
$Fr_M$	criterion characterizing specific features of flow in a bundle of helical tubes
$g$	gravity acceleration
$G$	mass flow rate of heat carrier
$K$	dimensionless coefficient of turbulent diffusion
$K_{Tg}^*$	parameter of thermal nonstationarity
$l$	length of a bundle
$Le$	Lewis number
$m$	bundle porosity with respect to heat carrier
$P$	static pressure
$P_n$	total pressure
$Pr$	Prandtl number
$q_v$	energy release in a bundle per unit volume of helical tubes ('solid phase')
$r$	radial coordinate

$Re$	Reynolds number
$s$	pitch of tube spiral
$T$	temperature
$u$	velocity
$x$	longitudinal coordinate.

## Greek symbols

$\alpha$	heat transfer coefficient
$\lambda$	thermal conductivity
$\lambda_e$	effective coefficient of turbulent thermal conductivity
$\nu_e$	effective coefficient of turbulent viscosity
$\xi$	coefficient of hydraulic resistance
$\Pi$	wetted perimeter
$\rho$	density
$\tau$	time.

## Subscripts

$b$	mean mass
$f$	fluid
$in$	inlet
$p$	at $P = \text{const.}$
$q.s.$	quasi-steady
$s$	solid phase
$un$	unsteady
$w$	wall.

case by the following system of equations

$$\rho_s C_s \frac{\partial T_w}{\partial \tau} = q_v - \frac{4\alpha m}{(1-m)d_e} (T_w - T) + \frac{1}{r} \frac{\partial}{\partial r} \left( r \lambda_s \frac{\partial T_w}{\partial r} \right) + \frac{\partial}{\partial x} \left( \lambda_s \frac{\partial T_w}{\partial x} \right), \quad (1)$$

$$\rho C_p \frac{\partial T}{\partial \tau} + \rho u C_p \frac{\partial T}{\partial x} = \frac{\partial P}{\partial \tau} + \frac{4\alpha}{d_e} (T_w - T) + \frac{1}{r} \frac{\partial}{\partial r} \left( r \lambda_e \frac{\partial T}{\partial r} \right) + \frac{\partial}{\partial x} \left( \lambda_e \frac{\partial T}{\partial x} \right), \quad (2)$$

$$\rho \frac{\partial u}{\partial \tau} + \rho u \frac{\partial u}{\partial x} = - \frac{\partial P}{\partial x} - \xi \frac{\rho u^2}{2d_e} + \frac{1}{r} \frac{\partial}{\partial r} \left( r \rho \nu_e \frac{\partial u}{\partial r} \right), \quad (3)$$

$$\frac{\partial \rho}{\partial \tau} + \frac{\partial (\rho u)}{\partial x} = 0, \quad (4)$$

$$P = \rho RT. \quad (5)$$

In deriving this system it is assumed that the transverse velocity components are much less than the longitudinal component,  $\partial P / \partial r = 0$ , and that the Mach number does not exceed 0.2. It is also assumed that the viscous dissipation and the term  $\partial(\rho \nu_e \partial u / \partial x) / \partial x$  can be neglected and that the porosity  $m$  is independent of the coordinates.

In order to close the system of equations (1)–(5), it is necessary to experimentally determine the dimension-

less relations for the quantities  $\lambda_e$ ,  $\nu_e$ ,  $\xi$ , and  $\alpha$ . Having assumed that the turbulent Prandtl ( $Pr_t = \rho \nu_e C_p / \lambda_e$ ) and Lewis ( $Le_t = \rho D_t C_p / \lambda_e$ ) numbers are equal to unity, the quantities  $\lambda_e$  and  $\nu_e$  can be expressed in terms of the effective coefficient of turbulent diffusion

$$\lambda_e = D_t \rho C_p, \quad (6)$$

$$\nu_e = D_t. \quad (7)$$

The aim of this work is to experimentally determine the coefficients  $\alpha$  and  $D_t$ , or in a nondimensional form

$$K = D_t / u d_e, \quad (8)$$

for unsteady behaviour of the process in the cases of an increase or decrease in time of the rate of heat release at the constant gas heat-carrier flow rate and their dependence on the criteria that determine the process. The coefficient  $D_t$  is determined by comparing the experimentally measured and theoretically predicted temperature fields of the heat carrier at each time instant  $\tau$ .

## 2. THEORETICAL DETERMINATION OF THE TEMPERATURE FIELDS

Since in this work consideration was given to the forms of the nonstationarity state associated only with a change in the heat flux released at  $G = \text{const.}$ , the system of equations (1)–(5) was reduced to the form

involving equations (1), (2) and (5) and also the motion and continuity equations in the quasi-steady approximation

$$\rho u \frac{\partial u}{\partial x} = -\frac{\partial P}{\partial x} - \xi \frac{\rho u^2}{2d_e} + \frac{1}{r} \frac{\partial}{\partial r} \left( r \rho v_e \frac{\partial u}{\partial r} \right), \quad (9)$$

$$G = 2\pi m \int_0^{r_k} \rho u r dr. \quad (10)$$

The temperature fields were calculated by means of numerical solution of equations (1), (2), (5), (9) and (10) with the following boundary conditions:

at the bundle inlet ( $x = 0$ )

$$\begin{aligned} T_w(r, 0, \tau) &= T_{w,\text{in}}(r, \tau), \\ T(r, 0, \tau) &= T_{\text{in}}(r, \tau), \\ u(r, 0, \tau) &= u_{\text{in}}(r, \tau), \\ P(r, 0, \tau) &= P_{\text{in}}(\tau), \end{aligned} \quad (11)$$

at the bundle exit (the condition of zero heat transfer)

$$\left. \frac{\partial T_w(r, x, \tau)}{\partial x} \right|_{x=l} = 0, \quad \left. \frac{\partial T(r, x, \tau)}{\partial x} \right|_{x=l} = 0, \quad (12)$$

on the bundle axis (the condition of axial symmetry)

$$\begin{aligned} \left. \frac{\partial T_w(r, x, \tau)}{\partial r} \right|_{r=0} &= 0, \quad \left. \frac{\partial T(r, x, \tau)}{\partial r} \right|_{r=0} = 0, \\ \left. \frac{\partial u}{\partial r} \right|_{r=0} &= 0, \end{aligned} \quad (13)$$

at the outer edge of the bundle

$$\begin{aligned} \lambda_s \left. \frac{\partial T_w(r, x, \tau)}{\partial r} \right|_{r=r_k} &= 0, \\ \lambda_e \left. \frac{\partial T(r, x, \tau)}{\partial r} \right|_{r=r_k} &= 0, \\ \left. \frac{\partial u}{\partial r} \right|_{r=r_k} &= 0. \end{aligned} \quad (14)$$

The initial conditions were found from the solution of the steady-state problem at time  $\tau = 0$ . In solving the system of equations (1), (2), (5), (9) and (10) with boundary conditions (11)–(14), the quantities preceding the derivatives were first averaged depending on the differentiation coordinates and were taken outside the differentiation sign and then were refined by iteration.

The heat transfer and energy equations were solved by the alternating direction method [9]. The numerical analogues of the equations were set up following an implicit scheme and were then solved by the factorization method. For the solution of the motion and continuity equations (in the form of an integral relation for the flow rate) use also was made of the implicit scheme and of the Simuni substitution technique [10]. Thus, the solution of the problem was split into two successive stages: the solution of the heat transfer equations and the simultaneous solution of the motion and continuity equations, which then were correlated via the state equations and iteration cycles.

For the numerical solution of the system of equations (1), (2), (5), (9) and (10) subject to boundary conditions (11)–(14), the grid  $r_i, x_i, \tau^v$  with the steps  $\Delta r, \Delta x, \Delta \tau$  was used. There was no constraint on the choice of the step in time, since the alternating direction method was used with an implicit scheme being stable in a wide range of the space-time steps. However, in order that a completely unsteady-state problem, described by the system of equations (1)–(5), could be solved, the step in time should satisfy the condition

$$\frac{\Delta \tau}{\Delta x} \leq \frac{1}{u+c}, \quad (15)$$

where  $c$  is the velocity of propagation of weak disturbances. An algorithm for the problem solution was realized in the form of a computational programme coded in FORTRAN and executed on the BESM-6 computer [11].

### 3. EXPERIMENTAL DETERMINATION OF TEMPERATURE FIELDS

An experimental investigation of the unsteady mixing of a heat carrier was carried out on a set-up shown in Fig. 1 by the method of heating the central group of a bundle composed of 37 helical tubes which were electrically insulated from the nonheated tubes with fibreglass fabric jacket over which a silicon-base lacquer was then applied. The bundle of 127 tubes had the length of 0.5 m. The helical oval-profiled tubes with the max. dimension of the oval  $d = 12.3$  mm and wall thickness of 0.2 mm had the tube spiral pitch  $s = 12d$  ( $Fr_M = s^2/dd_e = 220$ ). Uniform heat release in heated tubes was achieved by selecting the tubes on the basis of their ohmic resistance. The heat carrier temperature fields were measured in the outlet section of the bundle with the aid of a rack of chromel–alumel thermocouples, with the wire diameter of 0.1 mm, mounted on a traverse gear at the centres of the cells at the points  $r/r_k = 0.073, 0.128, 0.193, 0.265, 0.334, 0.408, 0.479, 0.624, 0.770, 0.916$ . In the outlet section of the bundle the large axes of the tube ovals were parallel to each other

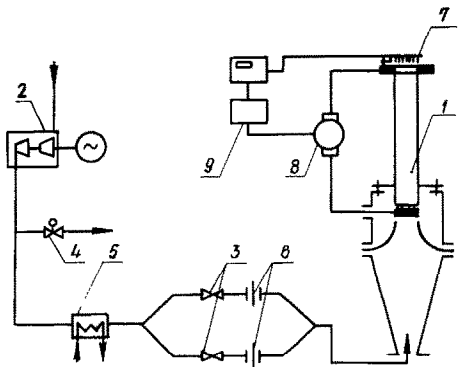


FIG. 1. Basic diagram of an experimental set-up: (1) test section; (2) turbo-compressor; (3) shut-off cock; (4) throttling cock; (5) refrigerator; (6) flow rate meter; (7) traverse gear with thermocouples; (8) generator; (9) automatic system for control and measurement.

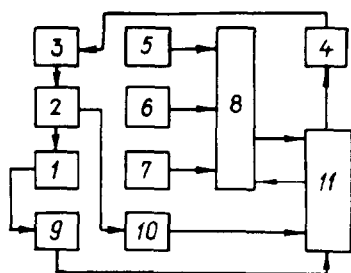


FIG. 2. Block diagram of an experimental set-up with an automatic system for control and measurement: (1) test section; (2) shunt; (3) generator; (4) power adjuster; (5) normalizer of the signals of thermocouples; (6) pressure transducer; (7) attenuator; (8) data converter; (9, 10) digital voltmeters; (11) measuring-computing complex IVK-2.

and formed continuous slit channels for the passage of heat carrier (air).

For the acquisition and processing of the experimental data in the case of unsteady-state heat transfer and mixing, an automatic system was used (Fig. 2) consisting of a measuring-computing complex IVK-2, direct current generator ANGM-90, pressure transducer KWS6A-5, generator power adjuster, and data converter. When the drive pulse is supplied from the data converter, the power adjuster exponentially changes the generator output power within certain limits with a specified time constant and voltage polarity. The measured temperatures, pressures, and voltages, transformed into an electric signal, are normalized by the amplifiers of the thermocouple signals, pressure transducer and attenuator, respectively, while the data converter records the voltages of signals with the polling frequency selected by an operator, and converts the analogue signals into the digital ones successively transmitting the data to the IVK-2 complex for their further processing and storage. The automatic system allows one to change the generator power in a stepwise manner or exponentially within 0–90 kW and vice versa. All of the probes are surveyed simultaneously in 40 channels. The fetching time spread is less than  $0.7 \mu\text{s}$ , the polling frequency is 1, 2, 5, 10, 20, 50 surveys  $\text{s}^{-1}$ . Numerical readout occurs with a frequency of 10 kHz. The experimental set-up with an automatic system of control, acquisition and processing of data made it possible, with a sufficient accuracy, to investigate the process of unsteady mixing in helical tube bundles.

#### 4. DETERMINATION OF THE COEFFICIENT $K$ . CORRELATION OF THE DATA OBTAINED

Typical changes in time of the heat flux and air temperature for the cases of sharp increase and decrease in loading are shown in Figs. 3(a) and (b). Experimentally measured air temperature fields in the cross section of the bundle at different time instants after a sharp increase in the intensity of heat release ( $\tau = 4, 6, 8, 10,$

12, 20, 30, 32, 36 s) are presented in Fig. 4 for  $Re = 8.9 \times 10^3$ . An increase in time of the intensity of heat release [Fig. 3(a)] occurred at a constant heat carrier flow rate. Figure 4 contains also, for the same time instants, the heat-carrier temperature fields predicted for different values of the coefficient  $K = D_i/ud_e$ . There is a good coincidence between the measured and predicted results but at different values of the coefficient  $K$  for different time instants. It is also seen that this coefficient decreases with an increase of time within the range of  $\tau = 0$ –10 s.

The numerical values of the coefficient  $K$  for each time instant are determined by a modified least squares method, i.e. a definite value of the coefficient  $K$  is assigned to each experimental point on the plots  $T = T(r, \tau, K)$  of Fig. 4 in accordance with the superposed grid of theoretical curves, and the squares of the deviations of each point  $\delta_i^2$  from these curves with the prescribed values of  $K$  are calculated.

Then the graph of the following relation is constructed

$$\sqrt{\sum_{i=1}^N \delta_i^2} = f(K), \quad (16)$$

where  $N$  is the number of experimental points, and the minimum of function (16) is determined which corresponds to the most reliable value of  $K$  at which the best agreement between the experimental and theoretical heat-carrier temperature fields is ensured.

The unsteady-state coefficients  $K_{un}$ , determined in this manner, are listed in Table 1. The relationship between these coefficients and time is very involved (Fig. 5) but it describes rather well all the data obtained at different values of  $Re$  ( $8.9 \times 10^3, 1.36 \times 10^4, 1.75 \times 10^4$ ). The coefficient  $K_{un}$  more rapidly attains a quasi-steady value,  $K_{q.s.}$ , than the heat-carrier temperature does [Fig. 3(a)]. The behaviour of  $K_{un}$  at the initial time instants agrees qualitatively with the behaviour of the unsteady-state heat temperature coefficient for a tube [7, 8] for the same type of nonstationarity. The latter coefficient attains the quasi-steady value also more quickly than the wall and heat carrier temperatures. This allows an assumption that the unsteady-state mixing in helical tube bundles is subjected to the effect of the same transfer mechanisms as the unsteady-state coefficient of heat transfer in channels [7, 8]. However, in a bundle of tubes the effect of the number  $Re$  within the ranges  $(8.9\text{--}17.5) \times 10^3$  and of the ratio  $(T_w/T_f)_{\max} = 1\text{--}1.37$  on the coefficient  $K_{un}$  is not observed (Fig. 5). The coefficient  $K_{un}$  characterizes a change in the heat-carrier temperature fields in the flow core on the scale of the helical tube bundle diameter in the solution of the conjugate problem of unsteady-state heat transfer in a homogenized formulation for the nonuniform field of heat release along the bundle radius, so that the unsteady-state coefficient  $K_{un}$  can be generalized with the aid of the Fourier number (the number of thermal homochronicity), which characterizes the relationship between the rate of change in the temperature field of the heat-carrier, its physical properties and dimensions

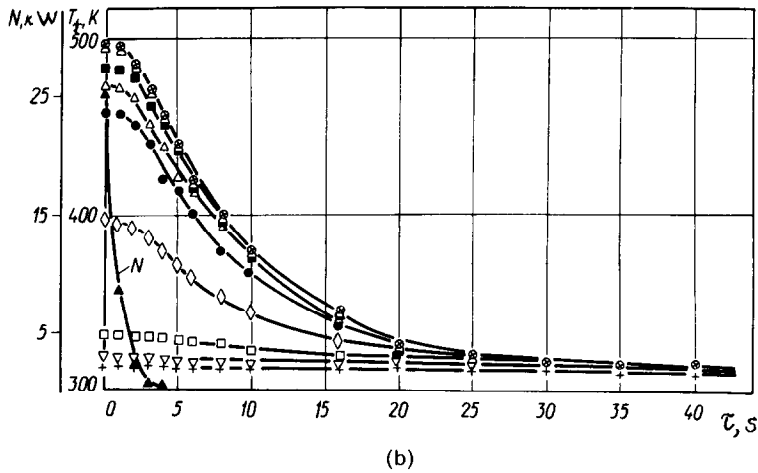
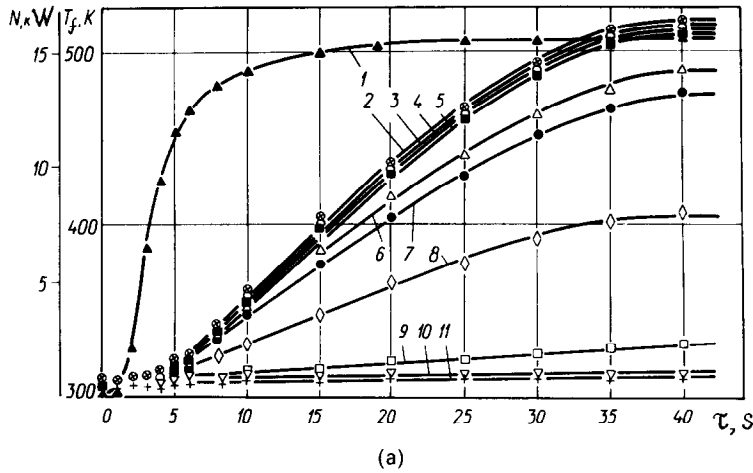


FIG. 3. Typical changes in the power and heat-carrier temperature in time after a sharp increase in heat loading at  $Re_b = 8.9 \times 10^3$  (a) and after a sharp decrease in heat loading at  $Re_b = 1.75 \times 10^4$  (b); (1) heat rating; (2–11) change in temperature at  $r/r_k = 0.07, 0.13, 0.19, 0.27, 0.33, 0.41, 0.48, 0.62, 0.77$ , and  $0.92$ , respectively.

of the flow region considered

$$Fo_r = \frac{a\tau}{d_k^2} = \frac{\lambda_r \tau}{C_p \rho_b d_k^2}, \quad (17)$$

and the following functional relation can be determined from experiment

$$\kappa = \frac{K_{un}}{K_{q.s.}} = \kappa(Fo_r). \quad (18)$$

It turned out that, on a sharp increase in the heat release rate at a constant heat-carrier flow rate, all the experimental data obtained for  $K_{un}$  and presented in the form of relation (18) (Fig. 5) are well described by the following interpolation relation [12]

$$\kappa = 0.81 \times 10^{-4} Fo_b^{-2} - 0.978 \times 10^{-2} Fo_b^{-1} + 1.21 \quad (19)$$

or

$$K_{un} = K_{q.s.} (0.81 \times 10^{-4} Fo_b^{-2} - 0.978 \times 10^{-2} Fo_b^{-1} + 1.21), \quad (20)$$

where  $K_{q.s.}$  are the quasi-steady values of the coefficient  $K$  determined by the relations derived in ref. [13].

Thus, a change in time of the coefficient  $K_{un}$  and of  $\kappa = K_{un}/K_{q.s.}$  (Fig. 5) can be explained by a change in the turbulent structure of the flow in the case of unsteady-state heating of a helical tube bundle resulting in the rearrangement of heat-carrier temperature fields. The action of this mechanism of transfer also accounts well for the specific features of unsteady-state heat transfer in channels studied in refs. [7, 8]. Taking into account the fact that there is the following relationship between the heat transfer coefficient  $\alpha$  and the temperature field in the flow

$$\alpha = \frac{\lambda(\partial T / \partial r)_{r=r_w}}{T_w - \left( \int_F \rho u T dF / \int_F \rho u dF \right)}, \quad (21)$$

the results obtained may be considered as confirming the hypothesis about the effect of unsteady-state boundary conditions on the flow structure [7]. Other

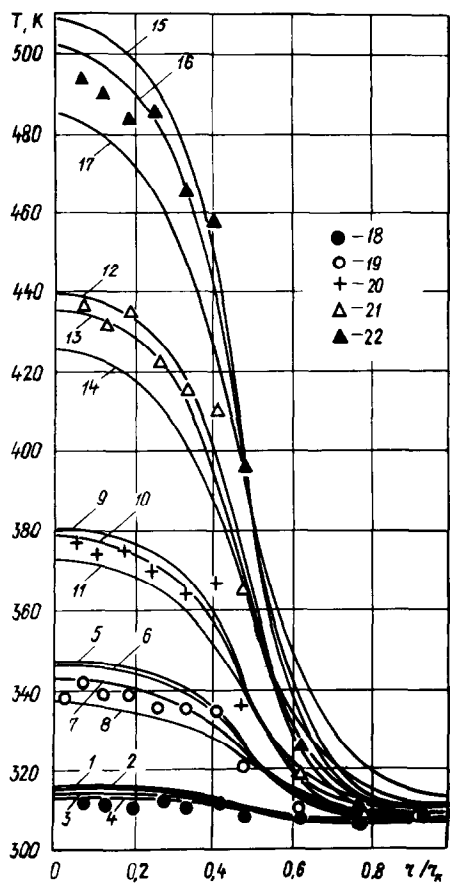


FIG. 4. Heat-carrier temperature fields in the outlet section of a helical tube bundle after an increase in heat loading at  $Re_b = 8.9 \times 10^3$  and at different time instants: (1–4) calculation at  $\tau = 4$  s for the coefficients  $K = 0.045, 0.06, 0.1, 0.2$ , respectively; (5, 6) same at  $\tau = 8$  s for  $K = 0.045, 0.06, 0.1, 0.2$ , respectively; (9–11) same at  $\tau = 12$  s for  $K = 0.045, 0.06, 0.1$ , respectively; (12–14) same at  $\tau = 20$  s for  $K = 0.045, 0.06, 0.1$ , respectively; (15–17) same at  $\tau = 32$  s for  $K = 0.045, 0.06, 0.1$ , respectively; (18–22) experimental data at  $\tau = 4, 12, 20, 32$  s, respectively.

mechanisms of transfer, which influence the coefficient  $K$  [4, 5, 13], depend to a lesser extent on the unsteady-state boundary conditions. Thus, an organized transport of heat carrier through the spiral channels of helical tubes is governed by the relative pitch of tube spiral  $s/d$  and is essentially independent of the nonstationarity parameters, while the convective transport on the scale of a cell, caused by a vortex exchange in the cross section between the wall layer and the flow core, can decrease, to a degree, the growth of turbulence at the first instants of time. It may well be that this is responsible for the coefficients  $K_{un}$  and  $\kappa$  having passed through a minimum (Fig. 5) before attaining the quasi-steady values—the fact which was not observed in the study of unsteady-state heat transfer in channels. As a whole, the heating of the wall increases the production of turbulence ( $\tau \leq 10$  s) resulting in the rearrangement of the temperature field not only in the wall layer, as was assumed in ref. [7], but also in the flow core (Figs. 5–7).

The use of homogenized flow model exerts a certain influence on the choice of the criteria to be determined while generalizing the data on  $K_{un}$ . In fact, in the case of a nonuniform field of heat release along the tube bundle radius, the resulting heat-carrier temperature field partially equalizes and the values of the temperatures  $T_w$ ,  $T_f$  and of the ratio  $T_w/T_f$  vary along the bundle radius. This leads to the uncertainty in the choice of the characteristic quantities  $T_w$ ,  $\partial T_w/\partial \tau$  in the formula

$$K_{Tg}^* = \frac{\partial T_w}{\partial \tau} \frac{1}{T_w} \sqrt{\frac{\lambda_h}{C_p g \rho_b u_b}}. \tag{22}$$

The coefficient  $K_{un}$  is a mean quantity for the bundle cross section where measurements of the distributions of  $T_f$  at each time instant were made (Figs. 5–7), while the quantities  $\alpha, \xi, u, \rho$  and others vary along the bundle radius. Moreover, when the temperature fields are considered in a homogenized formulation, the flow scale is the scale of  $d_k$ , rather than of  $d_e$ , which is used for

Table 1. Dimensionless effective coefficients of turbulent diffusion in the unsteady-state operational regime

Time (s)	$Re$			$Re$		
	$8.9 \times 10^3$	$1.36 \times 10^4$	$1.75 \times 10^4$	$8.9 \times 10^3$	$1.36 \times 10^4$	$1.75 \times 10^4$
	Sharp increase in power			Sharp decrease in power		
2	—	—	—	0.025	0.0275	0.026
4	0.2	0.2	0.2	—	—	—
5	—	—	—	0.03	0.04	0.043
6	—	0.125	—	—	—	—
8	0.078	0.08	0.075	—	—	—
9	—	—	—	0.059	0.0565	0.065
10	—	0.0575	—	—	—	—
12	0.057	—	0.053	—	—	—
13	—	—	—	0.064	0.060	0.065
20	0.052	0.054	0.046	—	—	—
30	—	0.060	—	—	—	—
32	0.0585	—	0.06	—	—	—
36	—	0.0575	—	—	—	—

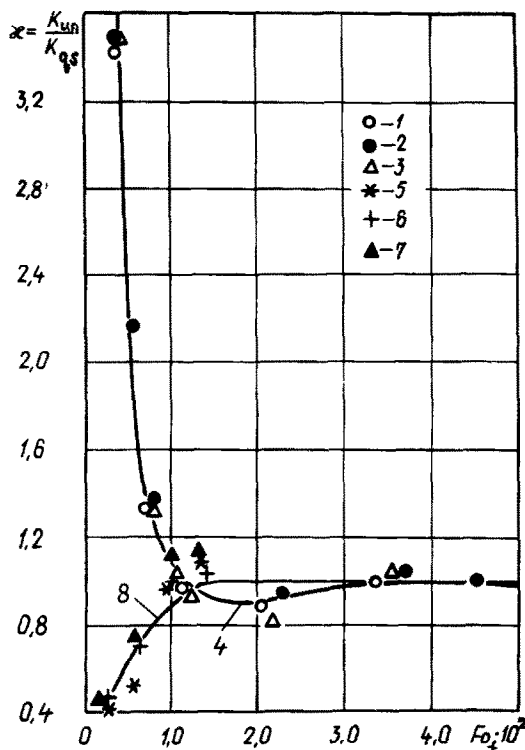


FIG. 5. Correlation between the relative unsteady-state coefficient of turbulent diffusion and the Fourier number: (1-3) experimental data for the case of a sharp increase in the heat release power at  $Re_b = 8.9 \times 10^3$ ,  $1.36 \times 10^4$ ,  $1.75 \times 10^4$ , respectively; (4) equation (19); (5-7) experimental data for the case of a sharp decrease in heat release power at  $Re_b = 8.9 \times 10^3$ ,  $1.36 \times 10^4$ ,  $1.75 \times 10^4$ ; (8) equation (23).

a one-dimensional description of unsteady-state heat transfer in a channel.

The results on the coefficient  $K_{un}$  for the regimes of a sharp decrease in the rate of heat release are presented in Figs. 6(a) and (b). As is seen from Fig. 5, a typical feature of this type of nonstationarity is a decrease in the intensity of the process of interchannel mixing at first time instants as compared with the quasi-steady operational conditions, thus testifying to the effect of the unsteady-state boundary conditions on the flow structure, which results in the rearrangement of heat-carrier temperature fields in time, and confirming the hypothesis suggested in ref. [7]. The character of variation of the coefficient  $K_{un}$  for this type of nonstationarity coincides with the character of variation of the coefficient  $\alpha$  in tubes [7, 8]. The nondimensional relation for the calculation of the coefficient in this case has the form [12]

$$\kappa = 0.454 \times 10^{-5} Fo_b^{-2} - 3.86 \times 10^{-3} Fo_b^{-1} + 1.24. \quad (23)$$

By analogy with the methods of the generalization of experimental data on unsteady-state convective heat transfer in channels in the case of a turbulent mode of flow [7, 8], it can be assumed that in a general case the experimental data on the unsteady-state coefficient of mixing can be presented in the form of the following

nondimensional relation

$$\kappa = \frac{K_{un}}{K_{st}} = \kappa(K_{Tg}^*, K_T, K_G, Re_f, T_w/T_f), \quad (24)$$

where the dimensionless parameter  $K_{Tg}^*$  is determined from equation (22). It allows for a change of the turbulent flow structure in the wall layer on a change of the wall temperature and therefore, as is shown in refs. [7, 8], characterizes a change in the thermal resistance between the wall and the flow under the conditions considered. This parameter also takes into account the effect of nonstationarity on the thermal resistance between the wall and the flow in a cell of a helical tube bundle. Since the unsteady-state coefficient of mixing should also depend on the thermal resistance between the cells, then, by analogy with equation (22), the effect of the unsteady-state variation of the flow temperature on this resistance can be taken into account by this dimensionless parameter as

$$K_{Tg}^* = \frac{\partial T_f}{\partial \tau} \frac{\sqrt{\lambda_b}}{T_f} \sqrt{ug\rho_b C_p}, \quad (25)$$

which allows for a change in the turbulent structure of the flow in a cell of a helical tube bundle with a change in its temperature. The mean mass flow temperature is used as  $T_f$ . Variations of  $T_f$  and of  $\partial T_f / \partial \tau$  are shown in Fig. 7.

The dimensionless parameter  $K_T$  characterizes the effect of the unsteady-state heat conduction taking place during equilization, due to the mixing, of temperature nonuniformities between the cells of the tube bundle and is expressed by the relation

$$K_T = \frac{\partial T_b}{\partial \tau} \bigg|_{r=0} \frac{d_k^2}{(T_{b_{tk}} - T_{b_{to}})|_{r=0} a_{be}} = \frac{\partial T_b}{\partial \tau} \bigg|_{r=0} \frac{d_k^2 C_p \rho_b}{\lambda_e (T_{b_{tk}} - T_{b_{to}})|_{r=0}}, \quad (26)$$

where  $a_{be} = \lambda_e / C_p \rho_b = D_t = K_{un} d_e u$ ;  $T_b|_{r=0}$  is the flow temperature at the centre of the helical tube bundle, i.e. at the place where the disturbance in heat release occurs;  $(T_{b_{tk}} - T_{b_{to}})|_{r=0}$  is a change of temperature at the centre of the helical tube bundle for the time of the unsteady-state process. The heat carrier effective thermal conductivity  $\lambda_e$ , entering into equation (26), is unambiguously connected with the coefficient  $D$ , and with the sought-after parameter  $\kappa$ , therefore in equation (26)  $\lambda_e$  can be replaced by the coefficient of molecular heat conduction  $\lambda_b$ . Then the parameter  $K_T$ , entering into equation (24), will be expressed by the relation

$$K_T = \frac{\partial T_b}{\partial \tau} \bigg|_{r=0} \frac{d_k^2}{\lambda_b (T_{b_{tk}} - T_{b_{to}})|_{r=0}} \frac{C_p \rho_b}{}, \quad (27)$$

which in fact is a derivative of the dimensionless flow temperature with respect to the Fourier number, equation (17).

In the case of the flow of gases in channels, the effect of the unsteady-state heat conduction on the processes

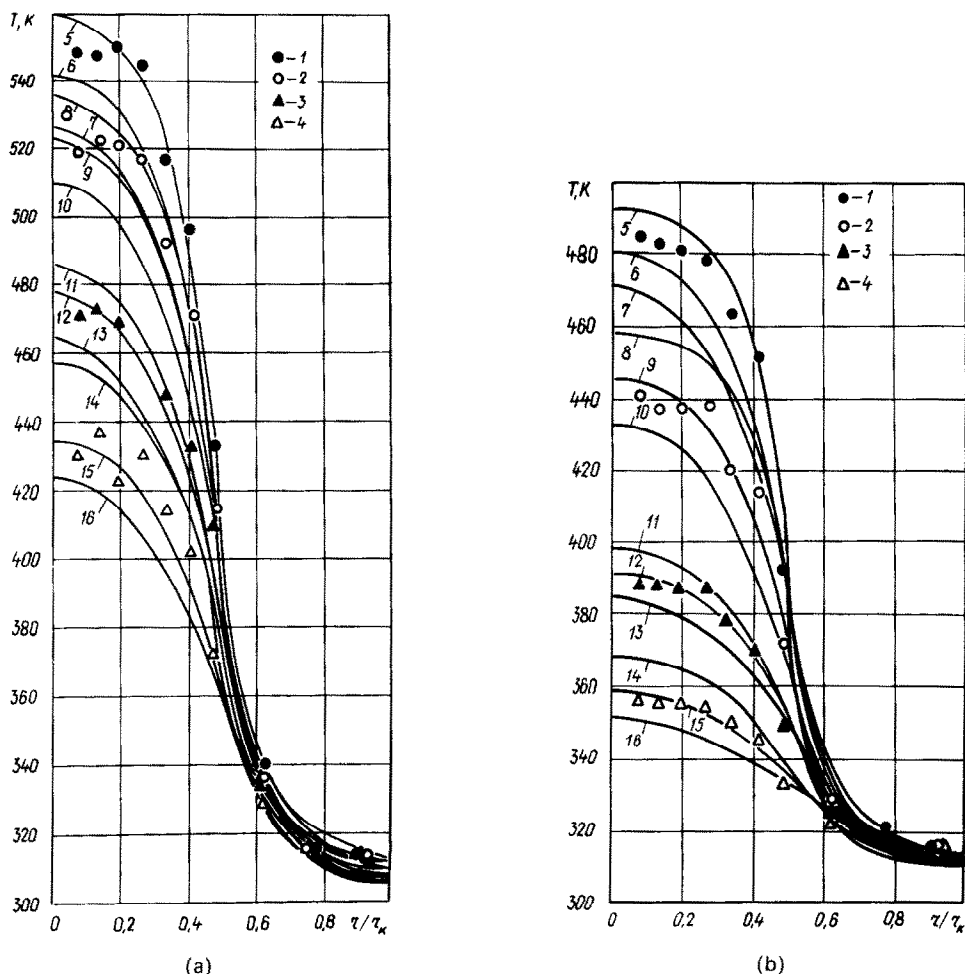


FIG. 6. Heat carrier temperature fields in the outlet section of a helical tube bundle after a decrease in heat loading at  $Re_b = 8.9 \times 10^3$  (a) and at  $Re_b = 1.75 \times 10^4$  (b); (1-4) experimental data at  $\tau = 2, 5, 9, 13$  s, respectively; (5-7, 8-10, 11-13, 14-16) calculated temperature fields at  $\tau = 2, 5, 9, 13$  s, respectively; (5, 8) at  $K = 0.02$ ; (6, 9, 11, 14) at  $K = 0.045$ ; (7, 10, 12, 15) at  $K = 0.06$ ; (13, 16) at  $K = 0.10$ .

of heat transfer is small [7, 8], since the gases have high thermal diffusivity coefficient,  $\alpha_b$ . Therefore, the parameter  $K_T$  can be eliminated from equation (24).

The dimensionless parameter,

$$K_G = \frac{\partial G}{\partial \tau} \frac{d_k^2}{G v_b} \quad (28)$$

entering into equation (24), characterizes the effect of a change in the heat-carrier flow rate on the process of unsteady-state mixing. When the flow rate is maintained constant in the course of the experiment, then  $K_G$  is eliminated from equation (24).

It is seen from the above that the functional relation (24) allows for a change, in the course of the unsteady-state process, both of the thermal resistance between the wall and the heat carrier flow in the bundle cell and of the thermal resistance between the cells. Once the change in the former thermal resistance has been taken into account by introducing the corresponding corrections into the heat transfer coefficient, occurring

in equations (1) and (2), with the aid of the empirical relation

$$\frac{Nu_{un}}{Nu_{q.s.}} = f\left(K_{Tg}^*, Re_b, \frac{T_w}{T_b}\right), \quad (29)$$

analogous in form to the relation for a circular tube [7, 8], and by determining  $\partial T_w / \partial \tau$  by the method of successive approximations, then the functional relation (24) is simplified to

$$\kappa = \frac{K_{un}}{K_{q.s.}} = \kappa\left(K_{Tg}^*, Re_b, \frac{T_w}{T_b}\right). \quad (30)$$

The experimental data on the  $\kappa$ -based increase in power within the range of the studied parameters with no effect from  $Re$  and  $T_w/T_b$  are correlated as

$$\kappa = \frac{K_{un}}{K_{q.s.}} = 1 + 4 \times 10^{22} (K_{Tg}^*)^6. \quad (31)$$

Using the procedure of determining  $\lambda_e$  from the measured heat-carrier temperature fields, the resulting



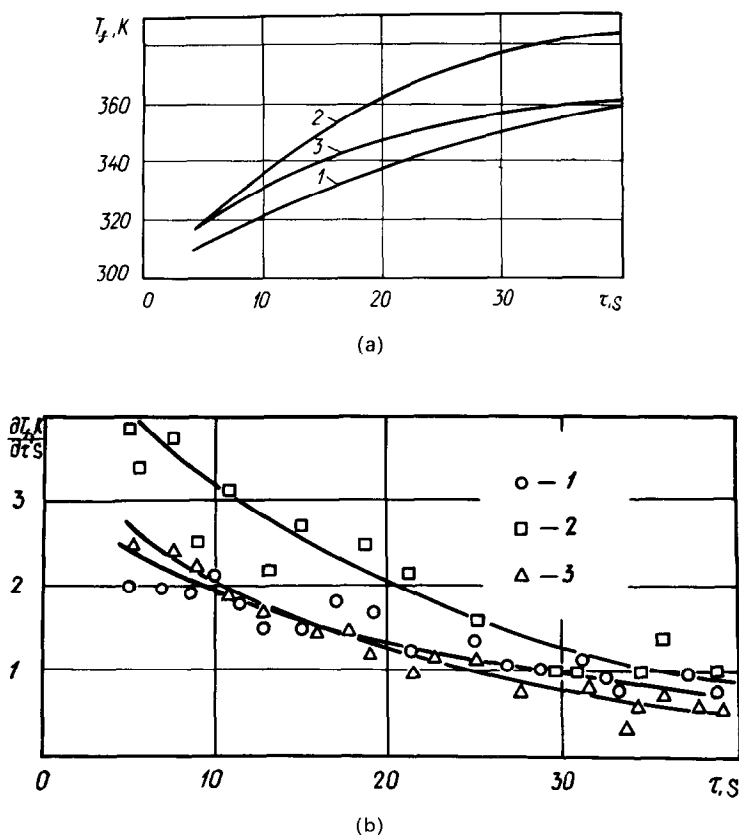


FIG. 7. Variation of mean mass temperature in a helical tube bundle (a) and of its gradient (b) in time after an increase in heat loading: (1, 2, 3) at Reynolds numbers equal to  $8.9 \times 10^3$ ,  $1.36 \times 10^4$ ,  $1.75 \times 10^4$ , respectively.

values of  $\lambda_e$  are the greater, the greater the prescribed values of the heat transfer coefficient  $\alpha$ , as is seen from equation (2). Therefore, when the quasi-steady values of  $\alpha$  are used, the values of  $\lambda_e$  and  $\kappa$ , obtained by this procedure, will be understated with an increase in time of the wall temperature, when the heat transfer coefficient is greater than its quasi-steady value, and overstated with a decrease in time of the wall temperature ( $\alpha_{un} < \alpha_{q.s.}$ ). However, as the respective estimates have shown, at the present experimental rates of change in the wall temperature the possible deviations of the unsteady-state heat transfer coefficient from its quasi-steady value is much smaller than the error of its determination. Therefore, for the solution of the systems of equations (1)–(5) the quasi-steady values of the heat transfer coefficient were used and the experimental data of the unsteady-state coefficient of mixing were correlated in the form of equation (30).

It should be noted that the derivation of the relation such as equations (29), (30) requires a very large number of experiments because all of the parameters, entering into this relation, are interrelated. For this reason, relation (18) was also used in the first stage of investigation for the particular types of unsteady-state effects and helical tube bundle parameters.

## 5. INVESTIGATION OF THE UNSTEADY-STATE HEAT TRANSFER COEFFICIENT

Investigation of the unsteady-state heat transfer coefficient was carried out on a bundle of 19 helical tubes. The tubes were heated by passing an alternating current and cooled by air. The unsteady-state thermal processes resulted from a jumpwise switching-on or switching-off of the electric loading at a constant cooling air flow rate. The unsteady-state heat transfer coefficient was measured in eight sections of the bundle, at the distances of  $x/d_e = 7$ –167 from the entrance, following the procedure of ref. [7] for which purpose measurements were made of: the air flow rate, the power of electric current passed through the bundle of tubes, the change in time of the wall temperatures of the tube bundle in its eight sections, the flow temperature at the inlet and outlet. The basic parameters varied in the experiments in the following ranges:  $Re_b = 5 \times 10^3$ – $5 \times 10^4$ ,  $T_w/T_b = 1$ –1.4,  $\partial T_w / \partial \tau = -50$ – $50 \text{ K s}^{-1}$ .

In the case of jumpwise switching-on of the electric load, the tube wall temperature increases in time and the increase is the greater, the farther the sections considered are away from the entrance. In this case, at

the initial time instants  $K_x = Nu_{un}/Nu_{a.s.} = 2-3$ . As the wall temperature stabilizes, the value of  $K_x$  tends to 1. On switching-off the heat load, the wall temperature decreases in time and the faster this happens, the higher the value of  $x/d_e$ . At the initial time instants  $K_x = 0.5-0.6$ , and then, as the wall temperature stabilizes,  $K_x \rightarrow 1$ .

Just like in refs. [7, 8], the processing of experimental data was carried out in the form

$$K_x = f(K_{Tg}^*, Re_b, T_w/T_b, x/d_e), \quad (32)$$

where the parameter of thermal nonstationarity have been determined by equation (22). As the processing of the experimental data has shown, the difference of  $K_x$  from unity is greater, the greater is  $|K_{Tg}^*|$ , while the influence of  $Re_b$  and  $x/d_e$  was not observed in the studied range of the parameters. On a change in the heat load, the dependence of  $K_x$  on  $K_{Tg}^*$  is also insensitive to the temperature factor  $T_w/T_f$ .

For an increasing heat load, the experimental data on the unsteady-state heat transfer coefficient are correlated as

$$K_x = 1 + (K_{Tg}^* \times 10^5) \frac{2.4}{(T_w/T_b)^{6.2}} \quad (33)$$

for  $Re_b = (1-5) \times 10^4$ ,  $T_w/T_b = 1-1.4$ ,  $K_{Tg}^* = 0-10^{-5}$ . For a decreasing heat load, the experimental data are correlated in the form

$$K_x = 1 - 0.412 [1 - \exp(1.9K_{Tg}^* \times 10^5)] \quad (34)$$

where  $Re_b = (1-6) \times 10^4$ ,  $T_w/T_b = 1-1.4$ ,  $K_{Tg}^* = -1.2 \times 10^{-5}-0$ .

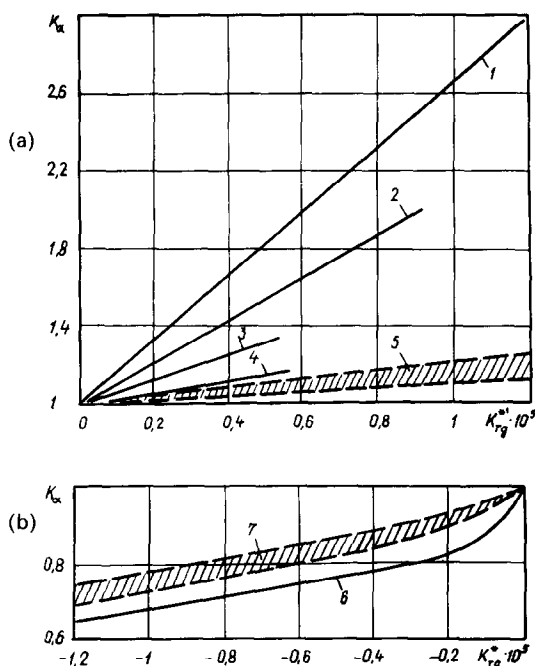


FIG. 8. The dependence of  $K_x$  on  $K_{Tg}^*$  after an increase (a) and decrease (b) of heat loading for helical tube bundles. (1-4) a bundle for  $T_w/T_b = 1-1.1, 1.1-1.2, 1.2-1.3, 1.3-1.4$  at  $Re_b = (1-5) \times 10^4$ ; (5, 7) tube,  $Re_b = (1-5) \times 10^4$ ,  $T_w/T_b = 1.1-1.5$ ; (6) a bundle for  $Re_b = (1-5) \times 10^4$ ,  $T_w/T_b = 1-1.4$ .

As is seen from Fig. 8, in the helical tube bundles at the same values of the thermal nonstationarity parameter  $K_{Tg}^*$ , the difference of  $K_x$  from 1 is greater than for a circular tube [7, 8].

## 6. CONCLUSIONS

(1) A good coincidence of the measured and calculated temperature fields testifies to the applicability of the homogenized flow model-based procedure developed for the solution of the conjugate problems of unsteady-state heat transfer with regard for the interchannel mixing of heat carrier in helical tube bundles.

(2) In helical tube bundles a great effect of the unsteady-state boundary conditions on the heat transfer coefficient has been revealed as compared with circular tubes under similar conditions. New trends discovered in the unsteady-state heat transfer and mixing and correlations developed for the calculation of the unsteady-state effective coefficient of turbulent diffusion and heat transfer coefficient allow the determination of the temperature fields in helical tube bundles for an axisymmetric problem in the case of nonuniform heat release field.

(3) Occurring on a sharp increase in the heat release intensity at a constant heat-carrier flow rate an additional enhancement of the process of equilization of the heat-carrier field nonuniformity, which results from a nonuniform unsteady-state heat release field, exerts a favourable effect on the performance capability of helical tube bundles, while a decrease in the intensity of transport processes on a sharp decrease in the heat load should be taken into account when the transitional regimes and closing of a heat exchanger are considered.

## REFERENCES

1. B. V. Dzyubenko and G. A. Dreitser, Investigation of heat transfer and hydraulic resistance in a heat exchanger with flow twisting, *Izv. Akad. Nauk SSSR, Energ. Transp.* **5**, 163-171 (1979).
2. V. M. Ievlev, B. V. Dzyubenko, G. A. Dreitser and Yu. V. Vilemas, In-line and cross-flow helical tube heat exchangers, *Int. J. Heat Mass Transfer* **25**, 317-323 (1982).
3. V. M. Ievlev, E. K. Kalinin, Yu. I. Danilov, B. V. Dzyubenko and G. A. Dreitser, Heat transfer in the turbulent swirling flow in a channel of complex shape, in *Heat Transfer 1982 Proc. of the Seventh International Heat Transfer Conference*, München, Vol. 3, General Papers. Hemisphere Publishing Corporation, Washington, pp. 171-176 (1982).
4. B. V. Dzyubenko, Study of the transport properties of a flow in a heat exchanger with spiral tubes, *J. Engng Phys.* **38**, 965-971 (1980).
5. V. M. Ievlev, B. V. Dzyubenko and M. D. Segal, Heat and mass transfer in a heat exchanger with a twisted flow, *Izv. Akad. Nauk SSSR, Energ. Transp.* **5**, 104-112 (1981).
6. B. V. Dzyubenko and V. M. Ievlev, Heat transfer and hydraulic resistance in the intertube space of a heat exchanger with flow twisting, *Izv. Akad. Nauk SSSR, Energ. Transp.* **5**, 117-125 (1981).
7. V. K. Koshkin, E. K. Kalinin, G. A. Dreitser and S. A. Yarkho, *Unsteady-state Heat Transfer*. Izd. Mashinostroenie, Moscow (1973).

8. G. A. Dreitser and V. A. Kuzminov, *Calculation of Heating and Cooling of Heat Pipelines*. Izd. Mashinostroenie, Moscow (1977).
9. B. L. Rozhdestvensky and N. N. Yanenko, *Systems of Quasi-linear Equations*. Izd. Nauka, Moscow (1978).
10. L. M. Simuni, Numerical solution for nonisothermal motion of a viscous liquid in a two-dimensional tube, *J. Engng Phys.* **10**, 58–61 (1966).
11. K. I. Pelageichenko and M. D. Segal, The technique of calculation of the nonstationary thermal hydraulic processes in a porous medium with internal energy release sources. Preprint No. 3581, Kurchatov Inst. of Atomic Energy, pp. 15 (1982).
12. B. V. Dzyubenko, M. D. Segal, L. A. Ashmantas and P. A. Urbonas, Nonstationary mixing of heat carrier in a heat exchanger with helical tubes, *Izv. Akad. Nauk SSSR, Energy, Transp.* **3**, pp. 125–133 (1983).
13. B. V. Dzyubenko, P. A. Urbonas and L. A. Ashmantas, Interchannel mixing of heat carriers in a bundle of spiral tubes, *J. Engng Phys.* **45**, 26–32 (1983).

#### TRANSFERT THERMIQUE VARIABLE ET MELANGE D'UN CALOPORTEUR DANS UN ECHANGEUR AVEC UN ECOULEMENT VRILLE

**Résumé**—Le problème de transfert thermique variable est considéré dans une formulation homogénéisée pour un mélange entre canaux dans un échangeur de chaleur avec tubes hélicoïdaux à profil ovale. Les champs de température axisymétriques dans l'espace entre tubes avec débit d'air constant ont été étudiés théoriquement et expérimentalement. Les procédures de calcul et d'expérience sont développées et on suggère des relations adimensionnelles pour les coefficients de transport, nécessaires pour la fermeture d'un système d'équations différentielles qui décrit l'écoulement instationnaire dans une grappe de tubes hélicoïdaux. L'effet du caractère instationnaire du mécanisme sur les coefficients de transport est dégagé.

#### INSTATIONÄRE WÄRMEÜBERTRAGUNG UND MISCHUNG EINES WÄRMETRÄGERS IN EINEM WÄRMETAUSCHER MIT DREHSTRÖMUNG

**Zusammenfassung**—Betrachtet wird das Problem der instationären Wärmeübertragung in einer homogenisierten Formulierung unter Berücksichtigung der Mischung zwischen den einzelnen Kanälen eines Wärmetauschers mit schraubenförmigen, ovalen Rohren. Die achsensymmetrischen Temperaturfelder im Raum zwischen den Rohren wurden bei zunehmender und bei abnehmender Energiefreisetzung und konstantem Luftstrom theoretisch und experimentell untersucht. Es werden die Vorgehensweisen für Rechnung und Experiment entwickelt und dimensionslose Beziehungen für die Transportkoeffizienten vorgeschlagen, welche für die Lösung eines Systems von Differentialgleichungen benötigt werden, das die instationäre Strömung in einem Bündel von schraubenförmigen Rohren beschreibt. Der Einfluß des nichtstationären Charakters des Prozesses auf die Transportkoeffizienten ist geklärt worden.

#### НЕСТАЦИОНАРНЫЙ ТЕПЛООБМЕН И ПЕРЕМЕШИВАНИЕ ТЕПЛОНОСИТЕЛЯ В ТЕПЛООБМЕННИКЕ С ЗАКРУТКОЙ ПОТОКА

**Аннотация**—Рассмотрена задача о нестационарном теплообмене с учетом межканального перемешивания в теплообменнике с витыми трубами овального профиля в гомогенизированной постановке. Теоретически и экспериментально исследованы осесимметричные поля температуры в межтрубном пространстве при увеличении и уменьшении мощности энерговыделения и при постоянном расходе воздуха. Разработаны методики расчета и эксперимента и определены критериальные зависимости для коэффициентов переноса, необходимые для замыкания системы дифференциальных уравнений, описывающей нестационарное течение в пучке витых труб.

Обнаружено влияние нестационарности протекания процесса на коэффициенты переноса.